High-Q Factor ZnO-based Film Bulk Acoustic Resonator Devices

Giwan Yoon* and Linh Mai*

*Information and Communications University (ICU)

E-mail : gwyoon@icu.ac.kr

ABSTRACT

In this paper, we studied a ZnO-based film bulk acoustic resonator (FBAR) device fabricated on a specially designed multi-layerd Bragg reflector part. Very thin chromium adhesion layers (0,03um thick) were additionally deposited to improve the quality of the Bragg reflector and some thermal treatments were performed to improve the resonant characteristics of the device. At the operating frequency of ~2.7GHz, excellent resonant characteristics were observed in terms of return loss and quality factor, and effective electromechanical coupling coefficient. These findings are expected to be highly promising and effective for improving the performance of the FBAR devices at high frequency.

Keywords

Resonator, FBAR device, Thermal annealing, Adhesion

Ⅰ. Introduction

Resonators and filters based on bulk acoustic waves (BAW) and surface acoustic waves (SAW) are widely used in wireless communication systems, from customer electronics to military systems, where frequency control is required. Day by day, customers are demanding higher speed and larger bandwidths, smaller in size but cheaper in price. From the microwave device point of view, at the frequency of interests (0.5 6.0 GHz), thin film bulk acoustic wave resonator (FBAR) devices can be one of the excellent choices. The FBAR device technology can be fully integrated with the conventional complementary-metal-oxide semiconductor (CMOS) and radio frequency integrated circuit (RFIC) fabrication technologies, eventually allowing for the realization of a single-chip radio or a transceiver in the future [1-4].

Geometrically, the FBAR devices, one of the acoustic wave devices, consist of a piezoelectric film sandwiched between top and bottom metal electrodes. When an RF signal is applied across the device electrodes, it creates an acoustic wave propagating through the piezoelectric film and hence it produces a resonance [5]. Generally, the FBAR devices fabricated mostly using thin-film techniques are categorized largely into modes: the membrane (namely FBAR) and the mirror (SMR: solidly mounted resonator) types. When the propagation energy in the resonator is isolated on both sides by air (e.g., the piezoelectric material is suspended above the substrate), the device is called FBAR type. If the piezoelectric material is isolated from the substrate by a series of an acoustic reflector mirror, the device is called SMR type. The configuration of the membrane structure is supported by the edgesof the substrate. Due to the removal of a portion of the substrate, the strain in the film may lead to the breakage of the film. In addition, the main drawback of membrane may be in the complication of the device fabrication. Due to the robustness issues of membrane configurations, alternative new approachesto achieve an acoustic isolation from the substrate were introduced by an acoustic mirror [6, 7]. On the other hand, the SMR-type FBAR devices have some advantages such as small size, low insertion loss and less power consumption.

In the SMR configuration, the top surface of resonator may have a normal air or vacuum interface while the bottom is solidly mounted on a mirror of Bragg reflector (BR) structure. The BR plays a role in acting as a mirror to prevent any possible energy loss into the substrate from the resonating piezoelectric part, enabling the FBAR device to have high quality

factor (Q). Therefore, in addition to the piezoelectric film itself, the improvement of the multi-layered BR part is also considered important to further improve the resonant characteristics particularly for the SMR-type FBAR devices. A high quality BR fabrication seems critical to fabricate high quality factor (Q) devices. A high quality BR part can be made using multi-layered thin films with low and high acoustic impedance. At the interfaces between high and low impedance layers in the BR, a large portion of the wave may be reflected. And the analysis of the function of the BR structure in reflecting wave at the edges of the resonator was reported elsewhere [6]. There are two well-known materials preferred to be used in fabricating BR mainly because of the large ratio of high to low acoustic impedance (about 8:1 impedance ratio). Those materials are tungsten (W)-high acoustic impedance (101106 kg/m2s) and silicon dioxide (SiO2)-low acoustic impedance (13.1106 kg/m2s) [7, 8]. In addition, both materials are easy to be deposited, thus facilitating the device fabrication process.

Until now, some studies to improve the resonant characteristics of the FBAR devices have been mainly focused on the growth of high-quality piezoelectric films such as ZnO and AlN [9-11]. Also, the temperature variations and compensations in the FBAR have also been investigated [12, 13]. However, few studies have been reported on the methods to improve the quality of the tungsten/silicon dioxide (W/SiO2) multi-layered BRs, and the studies on the FBAR devices have very rarely been reported that can operate at the higher fundamental frequency, named the second-order resonant frequency. The FBAR device micromachining-technically fabricated with an air-gap operated at 2.95 GHz was made by S.-H. Kim et al. [14]. The research focused on only the fabrication technique of the device did not pay much attention on the performance of the device at such high resonant frequency. In addition, the device did not show a high return loss value (~ -18.91 dB at 2.95 GHz) and there was no report on the figure of merit (FOM) of the device. Recently, Wei et al. has demonstrated the fabrication of SMR-type FBAR device designed for 2.5 GHz [15]. They fabricated SMR-type devices consisting of a multi-layered molybdenum/titanium (Mo/Ti) BR and AlN material for the piezoelectric layer. Consequently, their best resonator devices have just exhibited -16.7 dB in return loss at 2.31 GHz. Moreover, the effective electromechanical coupling coefficient (K_{eff}^2) of 2.1% and Q of ~ 112 are reported.

In this work, we present a fabrication technique of ZnO-based SMR-type FBAR devices operating at second-resonant frequency of ~ 2.7 GHz and an improvement technique to fabricate high-quality FBAR devices. The SMR-type FBAR devices were fabricated on a specially designed BR part formed by inserting very thin chromium (Cr) adhesion layers between W and SiO2 layers. Conceptually, the Cr layer is added not only due to its good bond-forming abilities but also to its having the same crystal structure as the W material of the body-centered cubic (bcc) structure. Thus, the additionally inserted Cr layers (0.03um-thick) are considered to improve the multi-layered BR quality. Then, the FBAR devices with the structure of piezoelectric film (ZnO) sandwiched between top and bottom Al electrodes were fabricated on the BR part. In addition, various thermal treatments were performed to further improve the characteristics of the FBAR devices and their effects on the device characteristics were investigated. At the operating frequency of ~ 2.7 GHz, an optimum thermal condition was found to exist for the significant enhancement of device characteristics. Using both the specially designed BR part and the optimum thermal technique, the ZnO-based FBAR devices were fabricated and key device parameters were extracted for device evaluations.

II. Design and Experiments

Figure 1a, b and c show the schematic structure of the ZnO-based FBAR device in three-dimension structure, the scanning electron microscope (SEM) image and two top electroe patterns, respectively. The device consists of a multi-layered BR on Si substrate and a piezoelectric (ZnO) film positioned between the top and bottom Al electrodes. The bottom electrode was also designed to act as a floating ground plane with the thickness of 1.0 m.

The FBAR devices were fabricated on a 4-in., p-type Si wafer as follows. First, a multi-layered BR was prepared by sequentially depositing several thin film layers of SiO_2, Cr, W, SiO_2, Cr, W, and SiO_2. Those SiO_2 layers (0.6 μm thick) were deposited using a chemical vapor deposition

(CVD) technique. The Cr (0.03 μm thick) and W (0.6 μm thick) layers were deposited using a sputtering technique.

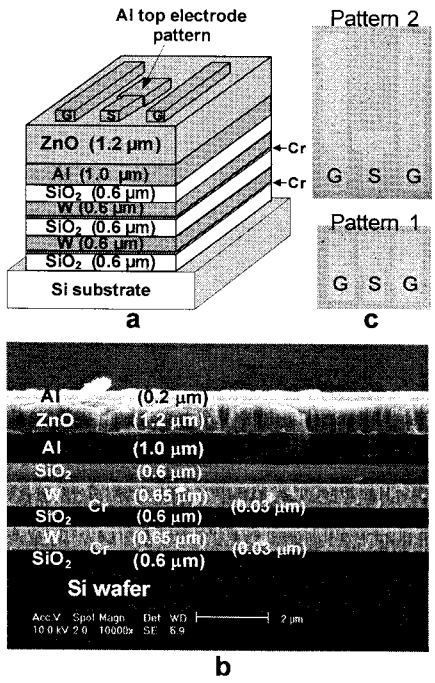

Figure 1: ZnO-based FBAR device: (s) three-dimensional schematic view, (b) SEM cross-sectional image and (c) two top electrode patterns 1 and 2 where the G-S-G is noted as ground-signal-ground.

Then, the 1.0-μm-thick Al bottom electrode was deposited on the Si wafer, followed by 1.2-μm-thick ZnO film deposition in a sputtering system. Subsequently, the Si wafer was divided into seven samples (S1 to S7). In order to investigate the thermal treatment effects, six samples (named S2 to S7) were thermally treated under various annealing conditions, whereas sample S1 was not thermally treated in order to use it as a reference sample. Immediately after the ZnO film deposition, the first thermal annealing (called inter-fabrication annealing) was carried out for six samples (S2 to S7), all at 200 °C for 120 minutes in argon (Ar) gas ambient in an electric dehydrate furnace (EDF) equipment. Then, the deposition and patterning of the top Al electrodes (0.2 μm thick) on the ZnO film completed the FBAR device fabrication. The top electrodes were patterned in ground-signal-ground (G-S-G) type in accordance with the coplanar probe tip pitch of 150 m. Finally, the seven FBAR device samples (S1 to S7) were obtained. Next, the second annealing (named post-annealing) was done for five samples S3 to S7 in the EDF equipment for 220, 250, 260, 280, and 300 °C for 120 minutes, respectively. Here, two different resonator layout patterns, 1 and 2 (with areas of 37500 and 40000 μm^2, respectively) were designed for the second-order resonant at ~ 2.5 GHz. The return loss (S_{11}) characteristics were extracted using a well calibrated cascade probe station and Agilent 8510C vector network analyzer. Besides, after the data collection, the sample S1 was cross-sectionally cut to get the real device SEM image (as shown in Fig. 1b). As a result, the thicknesses of all layers in the fabricated SMR-type FBAR deviceswere confirmed. Almost all the layers have shown the reasonably desired thickness values, but the SiO_2 layers were a little bit thicker than expected value (0.6um).

III. Results and Discussion

Figure 2a and b illustrate the return loss characteristics versus frequency for various thermal annealing conditions for the two resonators with top electrodes patterns 1 and 2, resonating at ~ 2.7 GHz. There are little shifts of the resonant frequencies in the fabricated devices. The S11 values of the three post-annealed resonators fabricated on the S3 to S5 samples show the same increasing trend in comparison to the S11 of resonators on the S1 and S2 up to 260 °C annealing temperature. But at higher temperatures ($\geq$ 280 °C), the S11 values of the resonators on the S6 and S7 samples were quickly dropped. Undoubtedly, there is an optimum thermal annealing temperature range (250-260 °C/120 minutes) for the significant enhancement of the S11 values of the devices. At the optimum annealing condition, the S11 values were -50.61 dB (at 250 °C) and -51.69 dB (at 260 °C) for the pattern 1 (Fig. 2a) and pattern 2 (Fig. 3b) of the resonators, respectively. All the extracted S11 values were summarized in Table 1.

Figure 3 shows the S11 values measured at the resonant frequency. By the inter-fabrication annealing process, the quality of the piezoelectric ZnO layer could be enhanced in several aspects such as: grain size, preferred c-axis, and interfacial adhesions between layers of ZnO and Al films, thereby enabling the sample S2 resonators to have better S11-characteristics than the sample S1 resonators. Besides, the appropriate post-

annealing process may have an impact on the sandwiched structure of the resonator (Al/ZnO/Al) therefore, any possibly existing physical imperfections in the film microstructures and some poor adhesions at interfaces between the ZnO layer and the Al layers are believed to be eliminated or reduced, leading to the improved performance of FBAR devices.

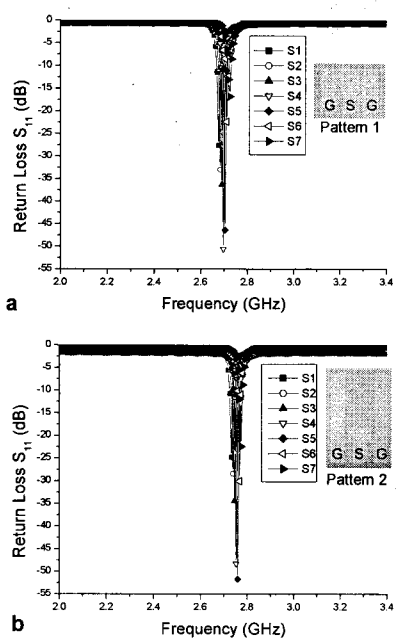

Figure 2: Return loss characteristics verus frequency for various thermal processes: (a) Pattern 1 and (b) Pattern 2.

Reportedly, the quality of the multi-layered BR part may have an impact on the FBAR characteristics [9, 10]. In the as-deposited SiO2/W BR, some physical defects may exist and/or some poor adhesions may occur at interfaces between the physically deposited films, hence degrading the device performances. The adhesion issues here can be resolved by inserting a very thin adhesion layer between W and SiO2 layers in the reflector. The inserted layers were formed by additionally depositing Cr films to enhance the adhesion property between W and SiO2 layers, and they were observed to have no deleterious effects on the BR structures or properties. In this work, the Cr adhesion layer is considered a reasonably good choice for the improvement of the adhesion between the W layer and SiO2 layer.

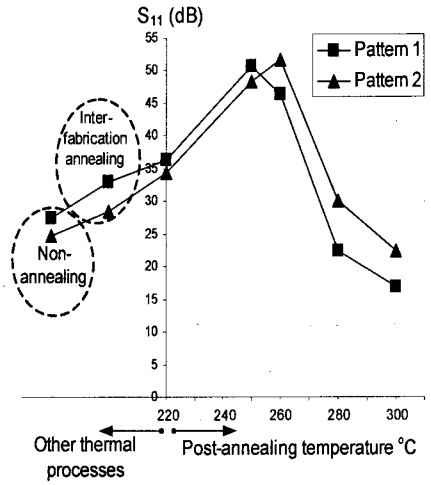

Figure 3: Comparison of the measured S11 values at resonant frequency for all fabricated resonators.

The key parameters used to assess the performance of the FBAR devices are quality factors (Qs/p) [6] and effective electromechanical coupling coefficient (K^2_{eff}) [16]. The Q-factor is a measure for the resonator loss in series and parallel resonant values. Based on the definition reported elsewhere [17], the series/parallel resonant Q-factors (Qs/p) were calculated as follows:

$$Q_{s/p} = \frac{f_{s/p}}{2}\left|\frac{d\angle Zin}{df}\right|_{f=f_{s/p}} \quad (1)$$

According to (1) that uses the local extrema in the slope of the input impedance phase ($\angle Zin$) as a function of the frequency for the resonator patterns 1 and 2, the series and parallel frequencies (fs and fp) and the slope of $\angle Zin$ as a function of the frequency are obtained. The effective electromechanical coupling coefficient indicates the strength of the piezoelectric interaction. It is determined from the formula below:

$$K^2_{eff} = (f_p^2 - f_s^2)/f_p^2 \quad (2)$$

As a result, the values of FOM of the FBAR devices were achieved and shown in Table 2.

It is clearly demonstrated that the post-annealed FBAR devices have larger Q-factors as compared to those with the non-annealed ones. Especially, the devices (S4 and S5) with the optimum post-annealing condition (at 250-260 ºC/120 minutes) have shown relatively higher Q-factors for all resonator patterns.

TABLE 1: Return loss values of electrode patterns

Sample	Return loss S11 (dB)	
	Pattern 1	Pattern 2
S1(non-annealing)	-27.56	-24.76
S2(inter-fabrication annealing 200℃)	-33.00	-28.41
S3(post-annealing 220℃)	-36.30	-34.39
S4(post-annealing 250℃)	-50.61	-48.30
S5(post-annealing 260℃)	-46.43	-51.69
S6(post-annealing 280℃)	-22.39	-30.05
S7(post-annealing 300℃)	-16.91	-22.45

TABLE 2: K_{eff}^2 factor and Q-factor for FBAR samples

Sample	Keff^2 factor(%)		Q factor			
	Pattern1	Pattern2	Pattern1		Pattern2	
			Qs	Qp	Qs	Qp
S1	2.14	2.14	6049	5848	5980	5724
S2	2.17	2.18	6889	6152	6129	5876
S3	2.16	2.15	7322	6258	6328	6186
S4	2.08	2.03	8214	6745	7945	6347
S5	2.04	1.97	8036	6581	8119	6325
S6	1.84	1.85	7362	6176	7082	6142
S7	1.86	1.86	6925	6072	7120	6247

Ⅳ. Conclusion

In this paper, we present the FBAR devices fabricated on top of the novel SiO2/Cr/W multi-layered Bragg reflector. Their resonant characteristics were investigated for various post-annealing treatments. With a process optimization, excellent return loss, good effective electromechanical coupling coefficient and high Q-factors were achieved at the resonant frequency of ~ 2.7 GHz.

Acknowledgment

This work was supported by the Korea Science and Engineering Foundation (KOSEF) grant funded by the Korea government (MEST) (No. R11-2005-029-06003-0)

References

[1] S. V. Krishnaswamy, J. Rosenbaum, S. Horwitz, C. Yale, and R. A. Moore, Microwaves RF,127 (1991).
[2] C. T.-C. Nguyen, L. P. B. Katehi, and G. M. Rebeiz, Proc. IEEE 86, 1756 (1998).
[3] L. Elbrecht, R. Aigner, C.-I. Lin, H.-J. Timme, IEEE MTT-S Digest, 395 (2004).
[4] J. F. Carpentier, et al., IEEE Int. Solid-State Circuits Conf., 394 (2005).
[5] S.V. Krishnaswamy, J.F. Rosenbaum, S.S. Horwitz, and R.A. Moore, IEEE MTT-S Dig., 153 (1992).
[6] K. M. Lakin, G. R. Kline, K. T. McCarron, IEEE Trans. on Microwave Theory and Tech. 41, 2139 (1993).
[7] K. M. Lakin, G. R. Kline, K. T. McCarron, IEEE Trans. on Microwave Theory and Tech. 43, 2933 (1995).
[8] S. Marksteiner, G. Fattinger, R. Aigner, and Kaitila, U.S.Patent No. US 6933807 B2, Aug, 2005.
[9] M. Yim, D.H. Kim, D. Chai, and G. Yoon, IET Electronics Lett. 39, 1638 (2003).
[10] M. Yim,D.H. Kim, D. Chai, and G. Yoon, J.Vac. Sci. Technol. A 22, 465 (2004).
[11] D.H. Kim, M. Yim, D. Chai, and G. Yoon, IET Electronics Lett. 39, 962 (2003).
[12] K. M. Lakin, K. T. Mc.Carron, and J. F. McDonald, Proc. IEEE Ultrasonics Symp. 1, 855 (2000).
[13] S. L. Pinkett, W. D. Hunt, B. P. Barber, and P. L. Gammel, Proc. IEEE Ultrasonics Symp. 1, 823 (2001).
[14] S.-H. Kim, J.-S. Lee, H.-C. Chol, and Y.-H. Lee, IEEE Electron device letters 20, 113 (1999).
[15] C.-L. Wei, Y.-C. Chen, C.-C. Cheng, K.-S. Kao, Appl. Phys. A 90, 501 (2008).
[16] IEEE Standard on Piezoelectricity, ANSI/IEEE Standard 176-1987, 1988.
[17] S.H. Park, B.C. Seo, H.D. Park, and G. Yoon, Jpn. J. Appl. Phys. 39, 4115 (2000).